

Fig. 1: Photomicrographs of quartzite and granite from contact and regional metamorphism; crossed polars. (A) Weakly polygonal quartz, coarsened during contact metamorphism, and K-feldspar (Kf); (B) Locations of TEM foils cut across quartz grain boundaries and quartz-K-feldspar phase boundaries (broken arrows) and of serial sections (black solid arrows); Ballachulish contact (Scottish Highlands). (C) Sutured and flattened quartz grains from low-T regional metamorphism (Scottish Highlands). (D) Quartz (qtz) recrystallized between coarse magmatic quartz (Qtz) during low-T regional metamorphism, granite from the Northern Aare Massif (Central Alps).

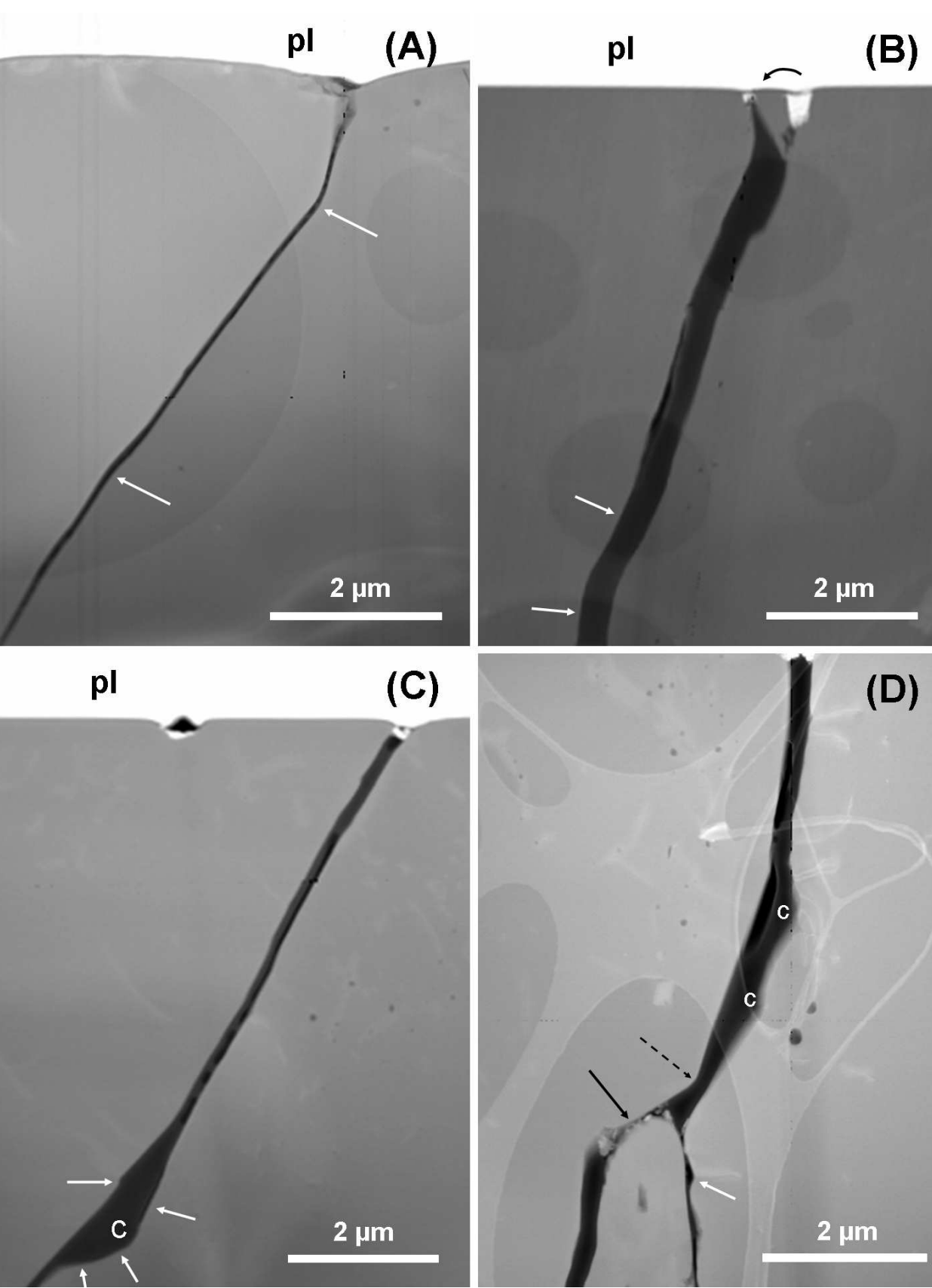


Fig. 2: HAADF TEM images of open sections of quartz grain boundaries. White bands (pl) are protective layers of platinum covering the thin-section surface prior to FIB milling. (A) Sample B10-86 from low-T region outside the Ballachulish contact. Arrows = short-distance curvature connecting straight grain-boundary segments. A small depression occurs where the grain boundary meets the thin-section surface. (B) Sample 4874-2 from the high-T part of the contact. The grain boundary is weakly segmented into µm-long straight sections (white arrows). A small grain fragment is rotated into the open grain boundary (curved black arrow), probably during thin-section polishing. (C) Same sample. A triangular cavity (c) is bound by straight segments (white arrows) of neighbouring quartz grains. (D) Same sample. Open grain boundary with cone-shaped cavities (c) and euhedral crystal faces connected by short-distance curvature (broken-line arrow). Small cavities are developed where dislocations meet the open grain boundaries (white arrow). On the crystal faces small quartz grains are grown (black arrow).

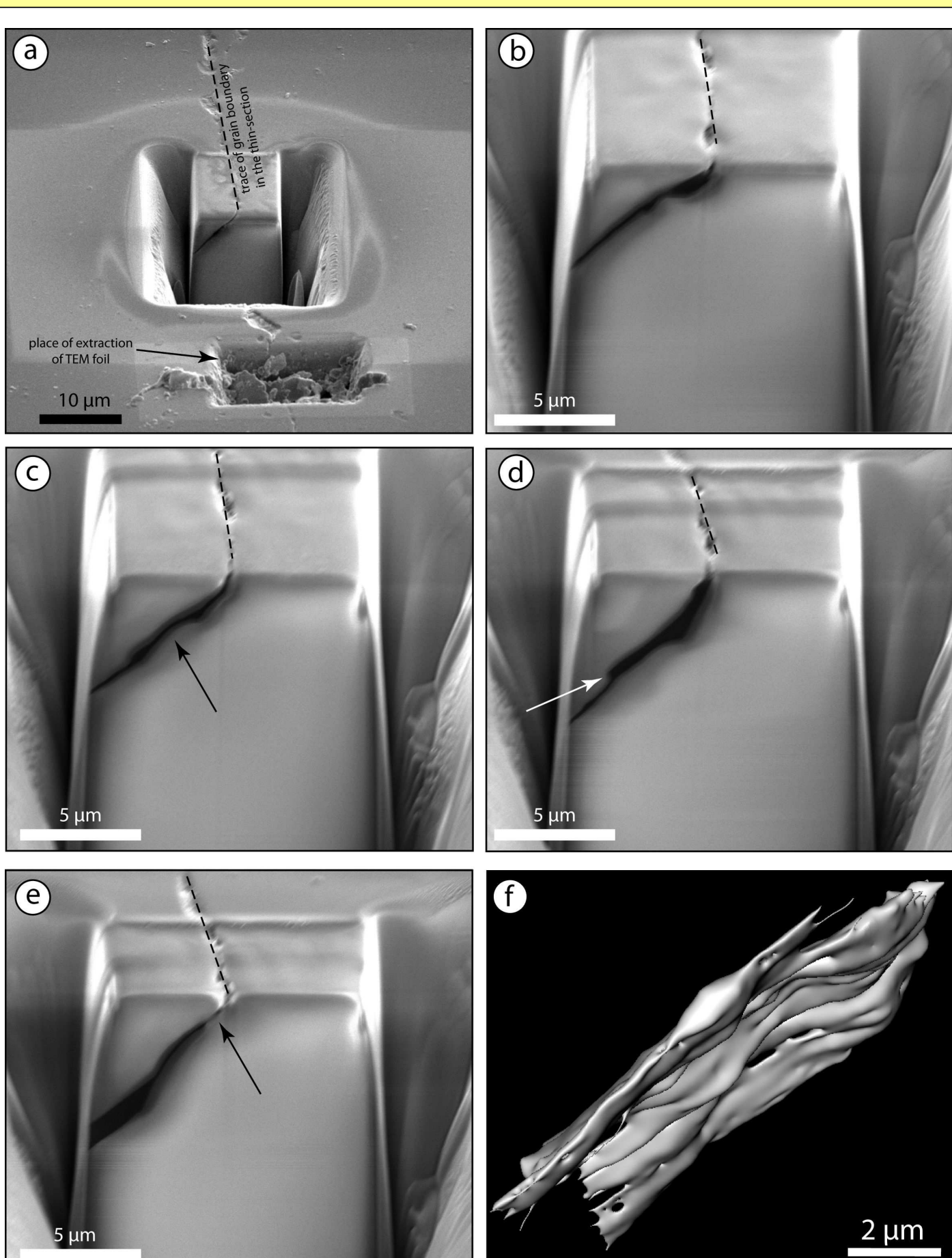


Fig. 3: Snapshots of the slice-and-view process along the boundary between two quartz grains. The image (a) indicates the initial slice-and-view setup with the frontal and lateral grooves excavated with the FIB, and also the place of TEM foil extraction. Grain boundary trace on the thin section is indicated by dashed lines on the images (a) to (e). Images (b) to (e) show the same grain boundary at different depths in 3D presenting different stages of grain openings and closings, with variation on the space between crystals (c). Locally the boundary is truncated and develops a small step with a different orientation of the general grain boundary (d). Image (f): 3D model of the space between the two grain boundaries based 100 slice-and-view images showing a "wave" behaviour of these structures in 3D. The view direction of this image is the same as of the snapshots and the animation. Sample 4874.

Open grain boundaries of quartz as fluid pathways in metamorphic rocks



Jörn H. Kruhl ⁽¹⁾, Richard Wirth ⁽²⁾, Luiz F.G. Morales ⁽²⁾

(1) Tectonics and Material Fabrics Section, Technical University Munich, 80333 Munich, Germany
(2) Helmholtz Centre Potsdam, GFZ German Research Centre for Geosciences, 14473 Potsdam, Germany



Grain and phase boundaries are one of the most important features of crystalline material. They affect rheological and petrophysical properties of rocks and provide information about their tectono-metamorphic history. Grain and phase boundaries are generally seen as dense, non-permeable structures (Hay and Evans, 1988; Heinemann et al., 2001). However, our present study shows that quartz grain boundaries from various geological environments are partially open to a large extent on the nanometre to micrometer scale. They form a connected network of porosity which possibly is a common phenomenon in low- to medium-grade metamorphic rocks.

TEM analyses coupled with SEM/FIB sequential imaging of quartz from a metamorphic contact aureole and from greenschist-facies regional metamorphism show that quartz grain boundaries are partly open. These voids can be separated in different types:

- (i) up to 500 nm wide openings with constant width,
- (ii) up to few microns sized cavities of different shapes, and
- (iii) dislocation-related nanometre-sized and cone-shaped depressions.

The opening probably results from reduction of cell dimensions during cooling below the diffusion threshold of quartz (ca. 300 °C). It is likely that the open grain boundaries form an at least partially connected network that generates permeability in the rock. In addition, the presence of voids along the grain boundaries may have important effect on petrophysical properties, such as strength, reactivity, elasticity, or storage capability.

Because the cell volume of any crystalline material is temperature dependent (Fei, 1995) and because thermal expansion of most of the minerals is anisotropic and only partly compensated by volume expansion during decompression (Levien et al., 1980), the process of grain-boundary opening can be expected to be common during cooling of all metamorphic and igneous rocks. In addition, the same process should also occur along phase boundaries as exemplified in this study and it should be expected along intra-crystalline cracks or cleavage planes. Since temperature dependent volume change is a relatively fast process it can be speculated if widths of open grain boundaries are even higher in volcanic rocks that crystallize over short periods of time and at much lower pressures, i.e., without much influence of decompression expansion. This would most prominently affect basalts of the oceanic crust, with all consequences for their physical properties.

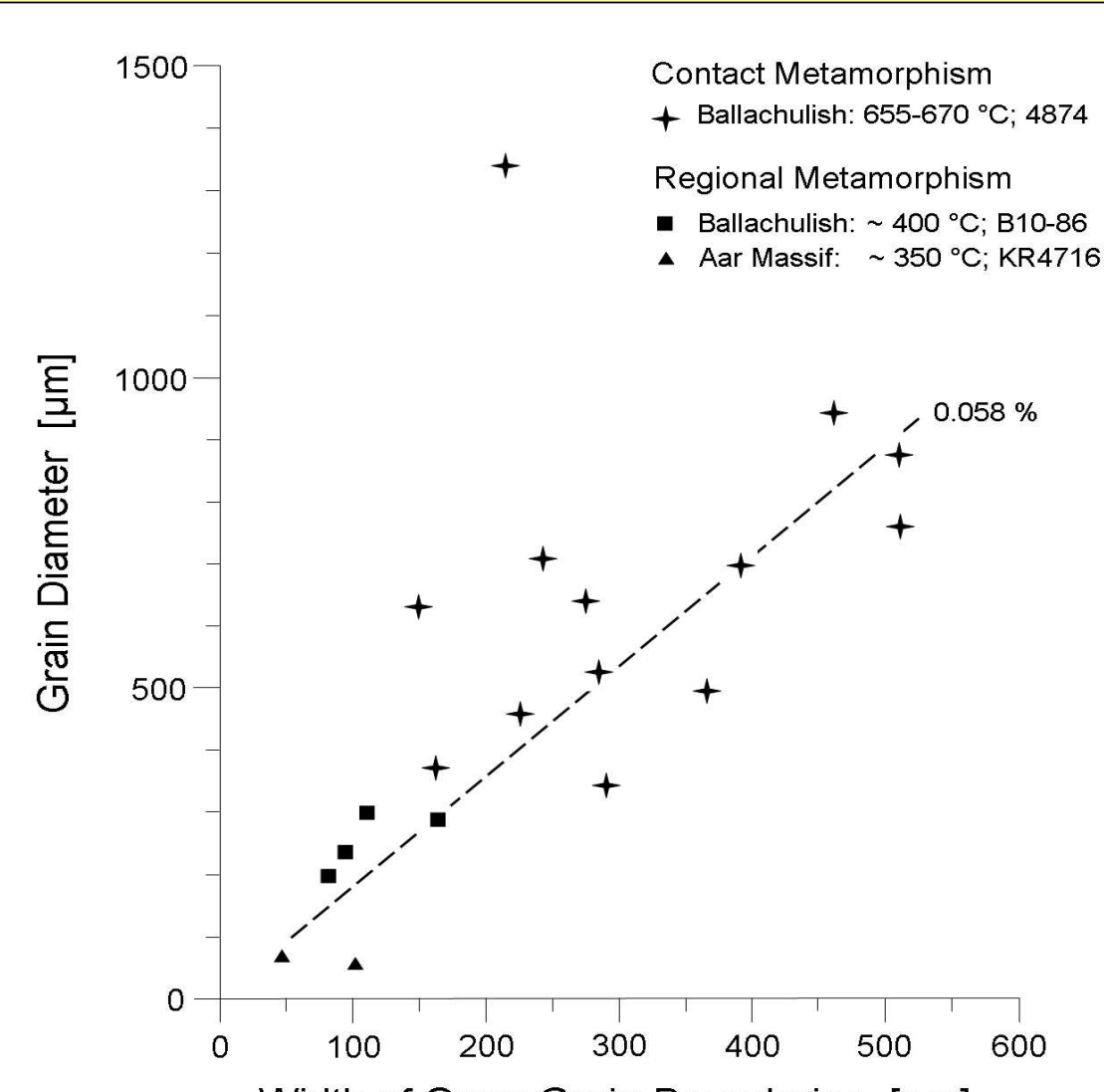


Fig. 7: Correlation between widths of 19 open quartz grain boundaries and grain diameters. Quartz from high-T contact and low-T regional metamorphism. The widths are determined based on TEM images (shown e.g. in figure 5) as perpendicular distance between opposite parallel grain-boundary segments, unless 'opening' oblique to the segments is indicated. The grain diameters are calculated as sum of the half diameters of the two neighbouring quartz grains, measured in thin section. The broken line indicates the average ratio of width of open grain boundary and grain diameter (0.058 %).

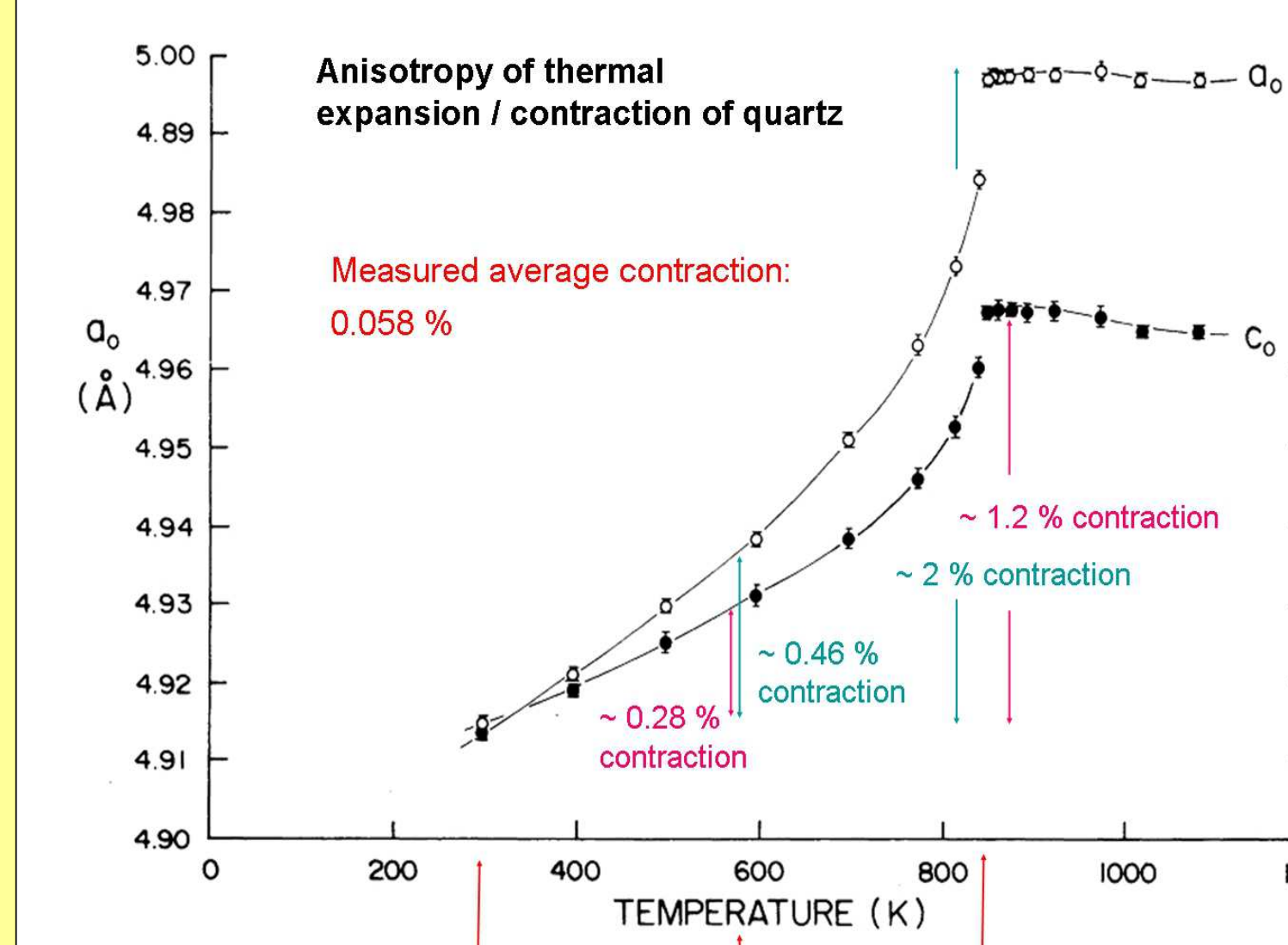


Fig. 8: Anisotropy of thermal expansion/contraction of quartz, with higher values parallel quartz-[a] compared to <c> (after Kihara, 1990). Rapid contraction at cooling below the high-low quartz transition is followed by decreasing contraction at further decreasing temperature. Contraction from 300°C (the diffusion threshold for quartz) to 25°C is ~ 0.46 % for [a] and ~ 0.28 % for <c>, i.e., still ~12-20 times higher than the measured average contraction of 0.058 %.

Temperature [°C]	575	300	25	Difference 300 – 25
[a] [Å]	4.9965	4.9363	4.9137	0.0226
<c> [Å]	5.4570	5.4198	5.4047	0.0151
1/2 ([a]+<c>) [Å]	5.2268	5.1781	5.1592	0.0189
Pressure [GPa]	0.25	0	Difference 0.25 – 0	
[a] [Å]	4.90638	4.9160	0.00962	
<c> [Å]	5.39761	5.4054	0.00779	
1/2 ([a]+<c>) [Å]	5.15197	5.1607	0.00873	
(a) Difference [Å] of [a] (300 – 25 °C) and [a] (0.25 – 0 GPa)	0.01298			
(b) Difference [Å] of <c> (300 – 25 °C) and <c> (0.25 – 0 GPa)	0.00731			
(c) Difference [Å] of 1/2 [a]+<c> (300 – 25 °C) and 1/2 [a]+<c> (0.25 – 0 GPa)	0.01017			
(a) – (c) = 0.00281 [Å] = 0.0572 % of [a] at 25 °C and 0 GPa				

Table 1: Cell dimensions of quartz at different temperatures and pressures, determined on the basis of data given by Kihara (1990) and Levien et al. (1980).

References:

- Fei, Y.W., 1995. Thermal expansion, in: Ahrens, T.J. (Ed.), Mineral Physics and Crystallography: A Handbook of Physical Constants, 2, 29-44. American Geophysical Union, Washington, D.C.
- Hay, R.S., Evans, B., 1988. Intergranular distribution of pore fluid and the nature of high-angle grain boundaries in limestone and marble. Journal of Geophysical Research 93, 8959-8974.
- Heinemann, S., Wirth, R., Dresen, G., 2001. Synthesis of feldspar bicrystals by direct bonding. Physics and Chemistry of Minerals 28, 685-692.
- Kihara, K., 1990. An X-ray study of the temperature dependence of the quartz structure. European Journal of Mineralogy 2, 63-77.
- Levien, L., Prewitt, C.T., Weidner, D.J., 1980. Structure and elastic properties of quartz at pressure. American Mineralogist 65, 920-930.

EGU General Assembly
Vienna 2012
Contribution 6307

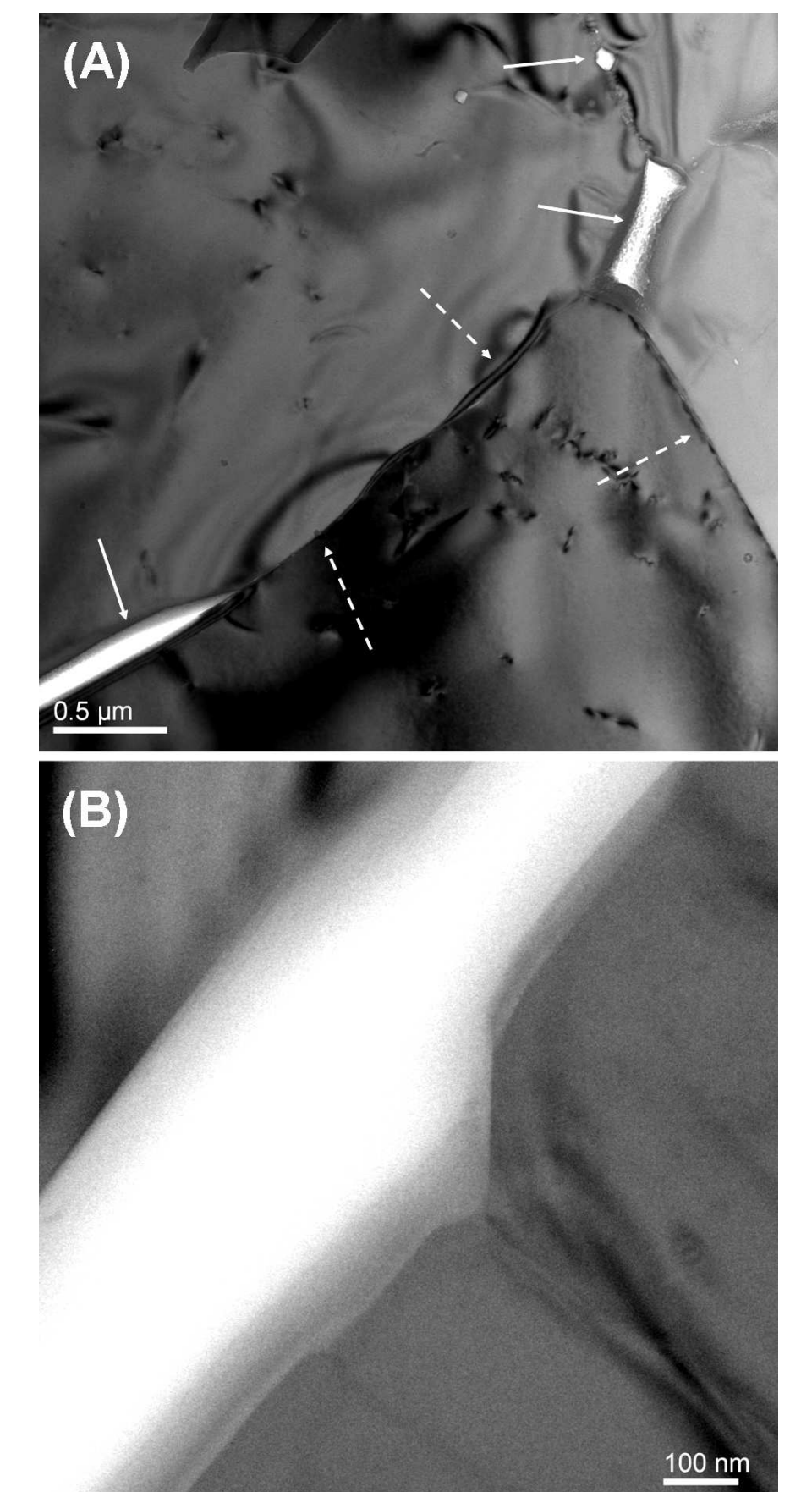


Fig. 4: TEM bright field images of quartz grain boundaries. (A) ~ 1 to 2 µm long and 100-200 nm wide open sections (arrows) of quartz grain boundaries from low-T regional metamorphism with several µm long straight closed segments (broken arrows). Sample B5-86B. (B) Cone-shaped euhedral depression developed where a dislocation line meets the surface of a quartz grain forming an open grain boundary. Sample 4874. White contrast = epoxy.

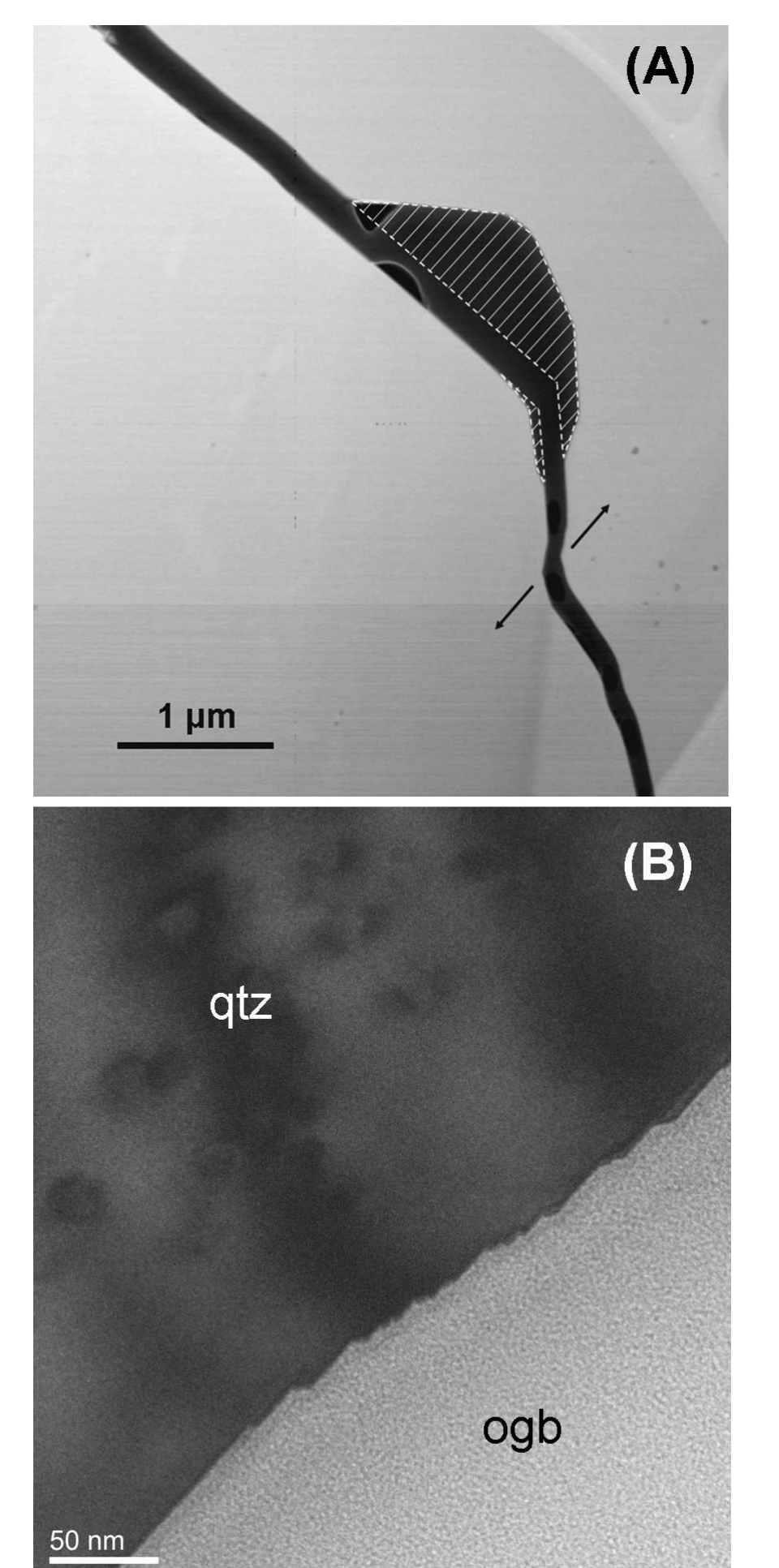


Fig. 5: (A) HAADF TEM image of an open quartz grain boundary with two additional polygonal cavities (hatched areas). Arrows = opening direction. Sample 4874. Dark contrast with bubbles is due to epoxy filling the open grain boundary. (B) TEM bright field image of grain surface at open quartz grain boundary section with prism-parallel wall, segmented by short probably rhombohedral steps. Prism-parallel orientation is determined by diffraction pattern. Sample 4874; ogb = epoxy-filled open part of the grain boundary.

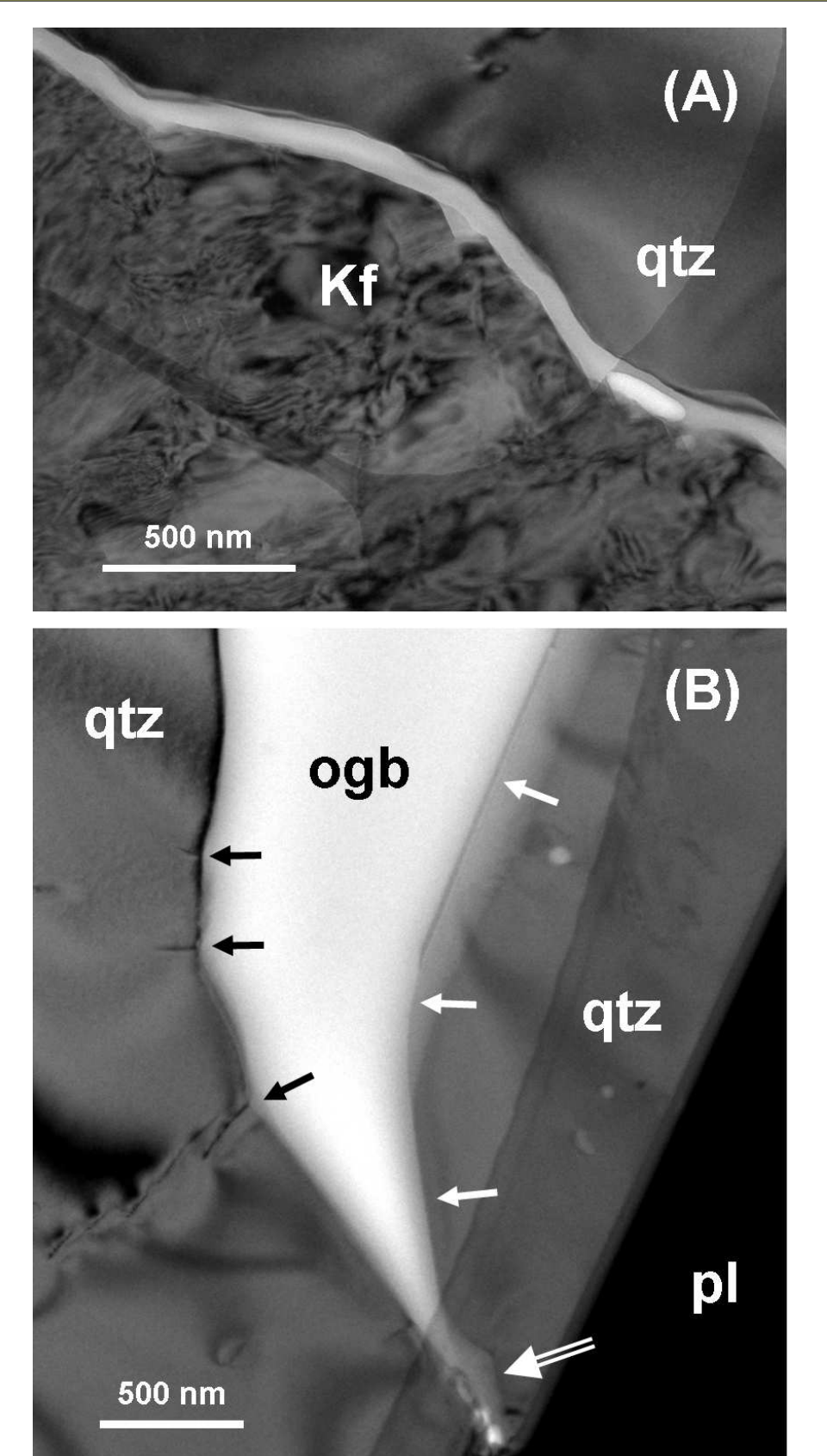


Fig. 6: (A) TEM bright field image of open ~100 nm wide quartz-K-feldspar phase boundary. The generally curved boundary is built by smaller partly straight segments. Sample 4874. (B) TEM bright field image of open quartz grain boundary (ogb). The ~150 nm wide grain boundary at the thin-section surface (white double arrow), covered by a protective layer of platinum (pl), opens towards the interior of the thin section. Large cavity shows euhedral shape (white arrows). Small cone-shaped depressions are developed where dislocations meet the crystal surface (black arrows). Sample 4874.